Egypt. J. Chem. Vol. 67, SI: M. R. Mahran, pp. **1713 - 1724** (2024)

Egyptian Journal of Chemistry

http://ejchem.journals.ekb.eg/

The Role of Tumor Microenvironment in Cancer Progression: A Pathological Approach to Biomarker Discovery

Fehan Falah Alhomidany[1], Abdulqader Ali Ahmed Muthaffar[2], Zahra Hajji Bohassan[3], Salman M. Muyidi[4], Nossiba Hussain Arkoubi[2], Afaf Wazen Alsulami[2], Effat Adnan Kadi[2], Yousef Sami Aldawaa[5], Mohammed Ibrahim Zuayr[6], Mohammad Ghaleb Al-amari[7], Wejdan Mohammed Alhazmi[8], Riyad Ibrahim Ali Zaidan[9], Badria Abdulmajeed Dakhilallah Almalki[10] and Sami Mohammed Alharbi[11]

[1]Comet General Hospital, Ministry of Health, Saudi Arabia
[2]General King Fahad Hospital Jeddah, Ministry of Health, Saudi Arabia
[3]Community Laboratory In Al-Hassa, Ministry of Health, Saudi Arabia
[4]Jazan Health Cluster, Ministry of Health, Saudi Arabia
[5]Wadi Al-Dawasir General Hospital, Ministry of Health, Saudi Arabia
[6]King Fahad specialty hospital, Ministry of Health, Saudi Arabia
[7](Hospital)/ Health Center Alhjrah, Ministry of Health, Saudi Arabia
[8]Hospital branch in Jazan, Ministry of Health, Saudi Arabia
[9]Jazan Health Cluster Chest Diseases Hospital in Jazan, Ministry of Health, Saudi Arabia
[10]Consultant - Medical Microbiology, Alyamama Hospital; , Ministry of Health, Saudi Arabia
[11]Forensic Medical Services Center, Ministry of Health, audi Arabia

Abstract

Background: The tumor microenvironment (TME) plays a crucial role in the progression of various cancers, influencing both tumor growth and therapeutic responses. Comprising multiple cellular components such as cancer-associated fibroblasts (CAFs), immune cells, blood vessels, and the extracellular matrix (ECM). Moreover, therapeutic interventions like chemotherapy and radiotherapy can further modify their composition, potentially affecting treatment outcomes.

Aim: This review aims to examine the role of the TME in cancer progression, focusing on its components and the potential of targeted imaging for therapeutic and diagnostic applications. It explores how understanding the TME's cellular heterogeneity and response to treatment could improve cancer management, particularly through molecular imaging.

Methods: We reviewed preclinical and clinical studies that investigated TME-targeted imaging agents, including radiotracers and biomarkers associated with CAFs, cancer stem cells (CSCs), ECM, and immune cells. Various imaging modalities, such as positron emission tomography (PET), magnetic resonance imaging (MRI), and single-photon emission computed tomography (SPECT), were explored for their potential in diagnosing and monitoring cancer progression.

Results: Studies identified specific biomarkers such as fibroblast activation protein (FAP) and collagen type I as key targets for imaging TME components. Radiotracers like [68Ga]Ga-FAPI-04 and [68Ga]Ga-FAPI-46 demonstrated improved diagnostic sensitivity and tumor-specific imaging compared to conventional markers like [18F]-FDG. These imaging agents enabled better visualization of TME-related factors.

Conclusion: Targeting the TME using advanced imaging techniques holds significant promise for enhancing cancer diagnosis, prognosis, and therapeutic monitoring. The integration of molecular imaging with TME biomarkers offers a path to more personalized and effective cancer treatments.

Keywords: Tumor Microenvironment, Cancer Progression, Molecular Imaging, Biomarkers, Cancer-Associated Fibroblasts, Imaging Modalities, Extracellular Matrix

1. Introduction

The tumor microenvironment (TME) is essential for the onset and advancement of multiple cancer types. It comprises a benign, complex cellular milieu that encompasses stromal elements (including the extracellular matrix, fibroblasts, mesenchymal stromal cells, osteoblasts, chondrocytes, and the basal membrane), non-stromal components (such as immune cells, blood vessels, and adipocytes), and microbiota [1]. Moreover, the functional diversity of the tumor microenvironment reflects its compositional complexity, exhibiting roles that are not wholly linear throughout tumor growth [2]. Moreover, therapeutic procedures like chemotherapy, radiation, and surgical resection may intensify the heterogeneity of the tumor microenvironment, as all treatment modalities affect its biological constituents both directly and indirectly [3, 4]. Recent findings indicate that chemotherapeutic drugs, intended to suppress cancer cell growth, also impact

*Corresponding author e-mail: falhomidany@moh.gov.sa (Fehan Falah Alhomidany)
Receive Date: 09 December 2024, Revise Date: 29 December 2024, Accept Date: 30 December 2024
DOI: 10.21608/ejchem.2024.342983.10950

stromal components, whereas radiotherapy modifies the tumor microenvironment composition, thereby affecting the efficacy of therapeutic radiation [5].

The relative quantity of tumor microenvironment (TME) components, in comparison to cancer cells, is a critical yet sometimes disregarded element, as TME components typically outnumber malignant cells in a fairly equal manner. The tumor microenvironment (TME) has considerable variability in cell types and functions, differing not only among various tumor types and individual cancer patients but even within distinct lesions of a single patient. Consequently, differentiating between the microenvironments of tumors and normal tissues is essential for the advancement of diagnostic instruments and chemotherapeutic drugs that precisely target tumor tissues. Understanding the evolution of the tumor microenvironment throughout tumor growth can aid in the development of stage-specific treatment options for cancer [6, 7]. Imaging the tumor microenvironment in longitudinal investigations of cancer progression, and therapeutic response is a burgeoning field in tumor microenvironment research, however it presents significant hurdles. Advanced imaging techniques designed to visualize dynamic alterations within the tumor microenvironment provide significant potential for improving cancer screening, diagnosis, and monitoring [8, 9].

The emergence of many imaging modalities and targeted tracers has enhanced the prominence of disease and cancer diagnosis. A variety of biomarkers inside the tumor microenvironment (TME) are accessible for imaging, and the capacity to visualize particular cells and physiological aspects of the TME can yield significant insights into cancer prognosis and treatment efficacy [12, 13]. This review will analyze several targets investigated for targeted imaging of the tumor microenvironment in both animal models and human research, employing diverse imaging modalities. We intend to provide a thorough overview of targets associated with cancer-associated fibroblasts, cancer stem cells (CSCs), the extracellular matrix, mesenchymal stromal cells, blood vessels, and the immune system, to improve comprehension of the intricate roles of the tumor microenvironment (TME) in tumor proliferation, considering the extensive diversity and complexity of biomarkers within the TME.

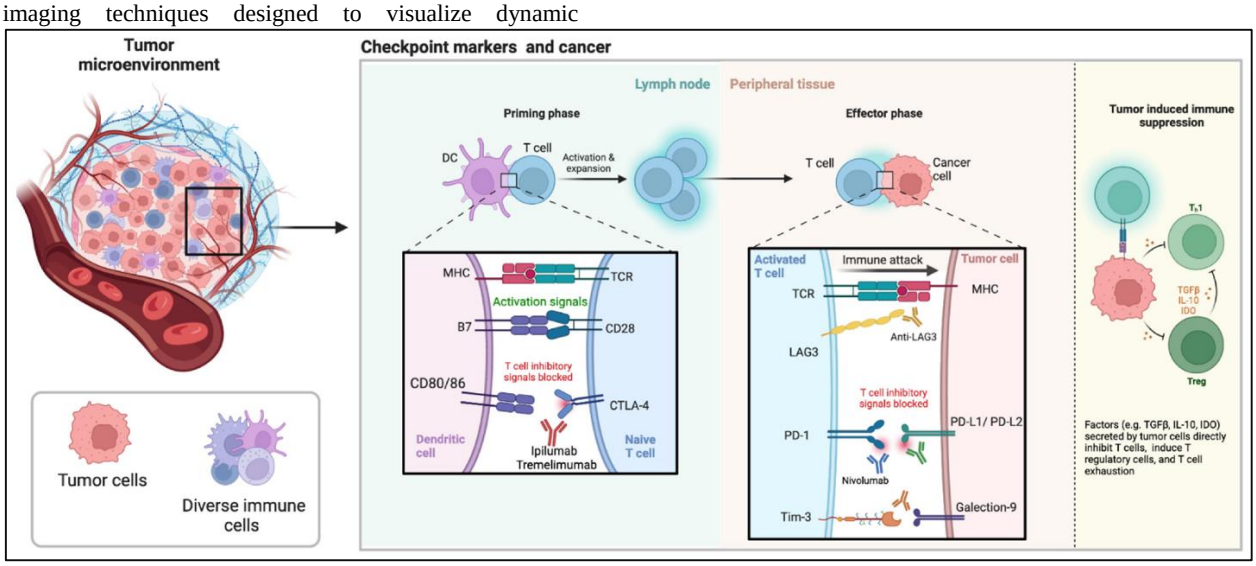

Figure 1: Tumor Microenvironment Markers.

Cancer-Associated Fibroblasts (CAFs):

Fibroblasts, prevalent mesenchymal cells in connective tissues, generally display non-epithelial, avascular, and non-inflammatory traits in their dormant condition. They may be temporarily triggered during tissue regeneration or wound healing, transforming into α-smooth muscle actin (αSMA)-reactive cells, referred to as myofibroblasts. Upon completion of their functions, they generally return to a dormant state [14]. In pathological situations including persistent inflammation or tissue damage, exemplified by the tumor microenvironment (TME), fibroblasts experience pathogenic activation [15]. Activated fibroblasts within the tumor microenvironment (TME) are designated as cancer-associated fibroblasts (CAFs). These CAFs represent a diverse population, distinguished by their proliferative characteristics and elevated secretory activity. This contrasts with the single-spindle-shaped myofibroblasts, which possess a more restricted lifespan [16]. CAFs exhibit phenotypic and functional diversity, which is affected by the origin of their precursor cells. Phenotypic heterogeneity in cancer-associated fibroblasts (CAFs) is seen both among different cancers (intertumoral heterogeneity) and within individual tumors (intratumoral heterogeneity), with specific genetic markers delineating these variations. Well-established indicators for cancer-associated fibroblasts (CAFs) comprise αSMA, vimentin, fibroblast activation protein (FAP), and fibroblast-specific protein 1 (FSP1 or S100A4) [17]. FAP is a type II transmembrane serine protease with endopeptidase activity and dipeptidyl peptidase capability. The overexpression of FAP is linked to unfavorable prognosis in multiple malignancies, including carcinoma, ovarian cancer, pancreatic cancer, hepatocellular carcinoma, and colon cancer. The FAP protein comprises a substantial extracellular domain, which includes a catalytic region likewise situated extracellularly [18].

Multiple research teams have created tiny compounds that specifically target FAP, notably enzyme inhibitors associated with macrocyclic chelators that function as radiotracers. [68Ga]Ga-FAPI-02 was evaluated in two xenograft mouse models, one expressing FAP and the other not, in addition to three human patients diagnosed with lung, breast, and pancreatic malignancies. The tumor uptake of [68Ga]Ga-FAPI-02 was swift in both animal and

human models, exhibiting substantial retention in mice for as long as 140 minutes. Thereafter, radioactivity was eliminated from the bloodstream, and the tracers were discharged through the kidneys, resulting in elevated tumor-to-organ ratios. Furthermore, the tracer demonstrated enhanced tumor absorption, reduced background radioactivity, and superior contrast relative to [18F]-FDG [19]. FAP-04 was synthesized to create a derivative of FAP-02 with a longer biological half-life, and its efficacy in positron emission tomography/computed tomography (PET/CT) for diagnosing liver cancer was compared to [18F]-FDG. The findings demonstrated that PET/CT with [68Ga]Ga-FAPI-04 markedly surpassed [18F]-FDG in the diagnosis of primary liver tumors and malignant lesions, especially in terms of sensitivity [20].

A multitude of preclinical and clinical investigations, documented on the clinicaltrials.gov website, have examined FAP-targeting compounds derived from FAP inhibitors to create radiotracers for diagnostic and therapeutic applications. The compounds comprise [68Ga]Ga-FAP-2286, [177Lu]Lu-FAP-2286, [68Ga]Ga-FAPI-46, and [68Ga]Ga-DOTA-FAPI. In a clinical trial, [68Ga]Ga-DOTA-FAPI-04, employing DOTA as a chelating agent, was evaluated against [18F]-FDG for PET/MRI imaging in patients with nasopharyngeal cancer. The findings indicated that although [18F]-FDG demonstrated a greater standardized uptake value (SUV) in primary tumors, the degree of parapharyngeal space invasion identified by [68Ga]Ga-DOTA-FAPI-04 was similar to that observed via MR imaging. Conversely, [18F]-FDG PET pictures did not agree with the associated magnetic resonance imaging (MRI) findings [29]. Furthermore, FAPI-46, a quinolone-derived compound radiolabeled with gallium-68, was evaluated for its safety, tolerability, and diagnostic precision in PET imaging. A clinical investigation with 43 patients suffering from bone or soft tissue sarcoma revealed that PET imaging utilizing [68Ga]Ga-FAPI-46 produced an 18.6% enhancement in tumor uptake relative to [18F]-FDG. This increase was associated with the degree of FAPI-46 tumor uptake in PET and the histological expression of FAP. Moreover, PET utilizing [68Ga]Ga-FAPI-46 demonstrated significant sensitivity and positive predictive value in the staging of sarcoma [23].

Molecular imaging radiotracers targeting FAP have demonstrated potential in preclinical and clinical assessments to enhance cancer diagnoses. Nonetheless, obstacles persist in their clinical utilization for cancer treatment, chiefly attributable to their swift clearance and inadequate retention within tumors. To resolve these difficulties, various modified FAP-targeted radiotracers conjugated with albumin binder-truncated Evans blue (EB) have been created. These tracers are derived from EB-FAPI-Bn, a variant of FAPI-02, and are radiolabeled with therapeutic radiometals, including lutetium-177. In biodistribution and SPECT imaging studies utilizing [177Lu]Lu-EB-FAPI-B1 in an animal model with U87MG tumors, the tracer demonstrated a minimal background signal and significant tumor accumulation, rendering it a promising candidate for therapeutic applications [28].

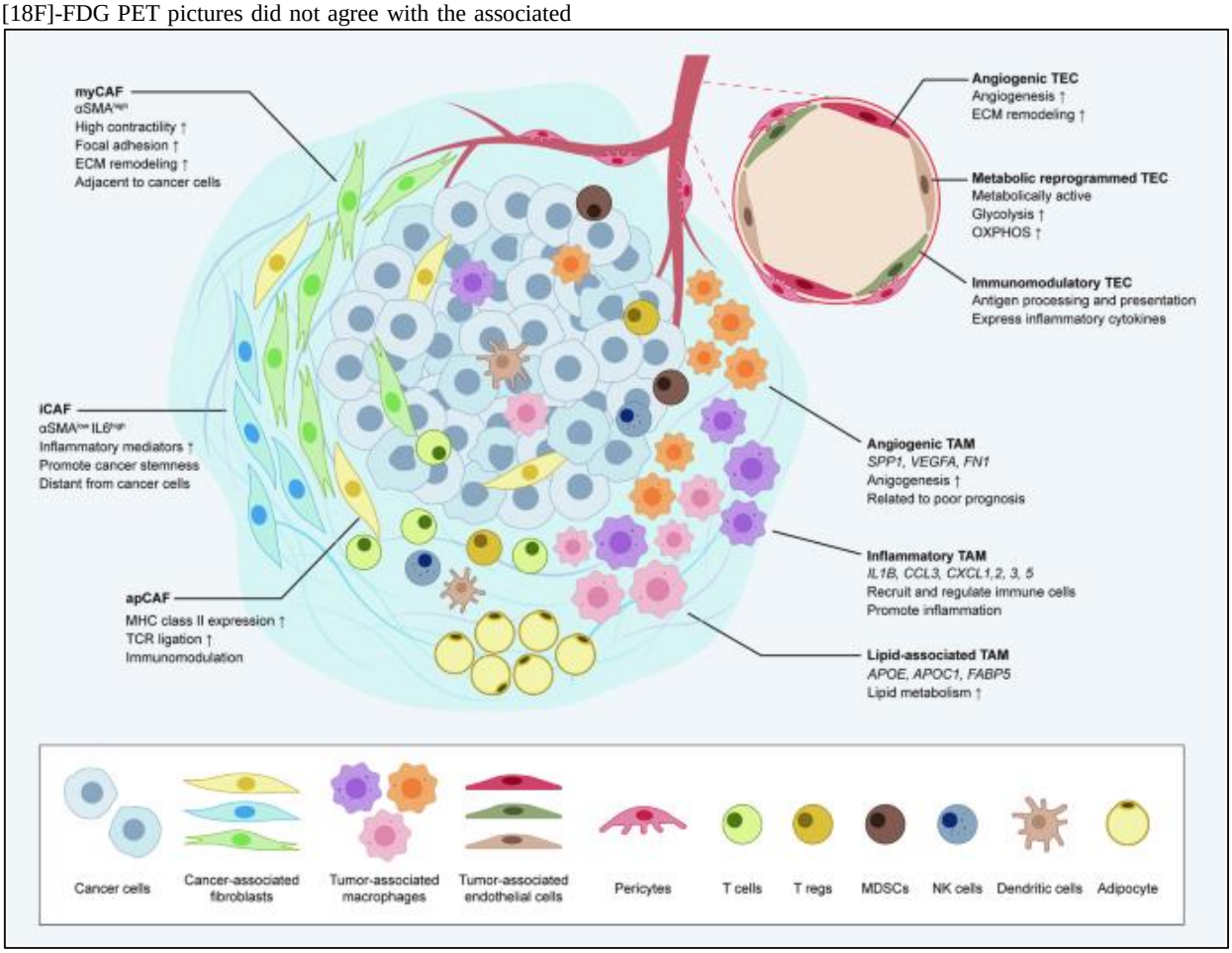

Figure 2: Tumor Microenvironment.

Investigated Agents and Imaging Modalities:

Several radiotracers have been explored for their potential in imaging the TME, particularly through PET/CT and PET/MRI modalities. For instance, [68Ga]Ga-FAPI-04 was assessed in a clinical trial involving 62 patients with non-Hodgkin lymphoma and 11 patients with Hodgkin lymphoma [21]. Similarly, [68Ga]Ga-FAPI-46 was evaluated in 15 patients suspected of having lung cancer or fibrotic interstitial lung diseases, and in genetically engineered mice models of idiopathic pulmonary fibrosis-like lung disease [22]. PET imaging using [177Lu]Lu-FAPI-46 and [225Ac]Ac-FAPI-46 was conducted in mice with PANC-1 xenografts [25], while in vivo experiments with AlF-[18F]-FAPT focused on tumor-bearing mice with A549-FAP cells [26]. Furthermore, PET and SPECT modalities have been employed in analyzing tumor-bearing mice with U87MG tumors and other cancer types, revealing significant diagnostic potential for imaging TME components [27, 28].

The Extracellular Matrix (ECM):

The extracellular matrix (ECM) is a non-cellular, three-dimensional framework that offers structural and biochemical assistance to cells, playing an essential role in tissue-specific support. The extracellular matrix (ECM) undergoes continuous remodeling via processes like wound healing and inflammation, facilitated by enzymes including matrix metalloproteinases (MMPs) and collagenases, alongside growth factors originating from fibroblasts [30]. The extracellular matrix (ECM) consists of two primary components: the basement membrane, which delineates epithelial cells from adjacent tissues, and the interstitial ECM, which fills extracellular spaces. Essential proteins in the interstitial extracellular matrix comprise fibrillar collagen, glycosaminoglycans, periostin, hyaluronan, tenascin C, and elastin. The ECM interacts with transmembrane integrins, facilitating the conversion of mechanical stresses into biochemical signals, a process termed mechanotransduction. Altered ECM stiffness, a characteristic of tumor advancement, influences multiple tumor behaviors including invasion, metastasis, growth, immune evasion, and angiogenesis [31].

Laminins, multiadhesive proteins located in the basal lamina, contribute to tumor invasiveness owing to their overexpression in malignancies. The YIGSR region of laminin, found on the β1 chain of laminin-1, has been the focus of imaging investigations. Liu et al. employed YIGSR coupled with rhodamine blue for fluorescence imaging in a mouse model carrying breast tumors. The findings indicated that tumors treated with the YIGSR-conjugated probe exhibited more robust and bright fluorescent signals than those treated with rhodamine blue [32]. Collagen, comprising 80-90% of the collagen in the human body, includes fibrillar types I, II, III, and V, which are released by fibroblasts and are the principal components of connective tissue in the extracellular matrix (ECM). Type I collagen is particularly abundant in fibrotic tissues, including those seen in pancreatic ductal adenocarcinoma (PDAC). CM-101, an imaging agent that targets collagen type I, was created for MR imaging in PDAC patients undergoing neoadjuvant chemoradiotherapy (CRT), which results in a dense collagen-rich extracellular matrix (ECM). In vivo imaging with CM-101 in a murine model demonstrated amplified MR signals in fibrotic tumor areas, facilitating distinct differentiation between fibrotic and remaining tumor tissues [34]. Investigating collagen breakdown can provide insights on the remodeling of malignant tissue. Collagen hydrolyzing peptides (CHP), including the modified sequence (GFO)9, provide non-invasive in vivo imaging of collagen degradation in cancer mice, offering an innovative approach to investigate pathological states such as cancer without requiring peptide preheating [35].

Fibronectin, produced predominantly by fibroblasts, plays a function in myofibroblast formation and is overexpressed in neovasculature and pathological angiogenesis. Qiao et al. conducted a study investigating MR imaging of extradomain-B fibronectin (EDB-FN), a biomarker that is overexpressed in pancreatic cancer, utilizing a peptide-fluorophore combination. The MRI utilizing MT218, a compound of the EDB-FN-targeting peptide, surpassed conventional MRI agents, offering enhanced contrast and improved tumor delineation in murine models of pancreatic cancer [37]. The extracellular matrix (ECM) comprises glycosaminoglycans (GAGs) and proteoglycans (PGs), which modulate cellular activity and matrix characteristics. Heparan sulfate (HS), a glycosaminoglycan, is overexpressed in neoplastic cells and facilitates malignant traits like proliferation, angiogenesis, and metastasis. Glypican-1 (GPC-1), a heparan proteoglycan, is associated with tumorigenesis, especially in pancreatic carcinoma. Gold nanoclusters (NCs) coupled with GPC-1 antibodies have been created as dual-modal imaging probes for the detection of pancreatic cancer. The Gd-Au-NC-GPC-1 probe exhibited in vivo fluorescence and MRI imaging capabilities, facilitating the identification of GPC-1-expressing cancer cells in prostate and pancreatic cancer models [40]. These investigations underscore the promise of targeting extracellular matrix components for diagnostic and therapeutic applications, particularly through imaging techniques to enhance the knowledge and treatment of cancer.

Tenascin-C (TNC-C), a protein that is overexpressed in solid tumors, represents a compelling target for malignancy imaging. Lingasamy et al. conducted a study utilizing a recombinant single-chain antibody targeting TNC-C (ScFv G-11) to investigate the biodistribution of fluorescein-labeled ScFv G-11, both conjugated with iRGD (an amino acid sequence) and as a standalone ScFv G-11 antibody, in U87-MG glioblastoma-bearing mice. Tissue slices were stained with vascular markers, and confocal imaging, together with an evaluation of tenascin-C positivity, was conducted. The findings indicated that the fusion of iRGD with ScFv G-11 improved the delivery of imaging agents to malignant lesions, due to iRGD's superior tumor homing and penetration capabilities [41]. Numerous enzymes in the meticizin superfamily, including disintegrin and metalloproteinase with thrombospondin motifs (ADAMTS), matrix metalloproteinases (MMPs), and disintegrin and metalloproteinases (ADAMs), which degrade collagen and elastin in the extracellular matrix (ECM), may become dysregulated during carcinogenesis. The breakdown by-products may activate many cellular pathways, potentially resulting in either protective or tumorigenic effects. MMPs, for example, cleave growth factors and receptors, such as EGFR [52]. Notwithstanding comprehensive research focused on creating therapeutic drugs that target MMPs, clinical trials have predominantly failed. This failure may be ascribed to the differing functions of MMPs and ADAMs in the ECM, which

fluctuate according to cancer type and grade. MMP8 serves a protective role in oral squamous cell carcinoma and is linked to a positive prognosis [54], while increased MMP8 levels in hepatocellular carcinoma correspond with a poor prognosis [55]. Recognizing the overexpression of metalloproteinases and their inhibitors can provide significant diagnostic insights for physicians in cancer detection.

Moreover, MMP9 and MMP2, categorized as gelatinases, are acknowledged as critical pro-tumorigenic agents in multiple cancer types. Historically, methods such as immunoassays and ELISA were utilized to identify these proteins. Recently, non-invasive imaging techniques aimed at metalloproteinases for tumor identification have attracted considerable attention [56, 57]. MMP2 and αvβ3 were targeted for imaging gastric cancer utilizing nanoparticles with dual imaging modalities: magnetic resonance and fluorescence. A nanoprobe was created by combining two elements: low molecular weight heparin (LMWH) modified with quantum dots and low molecular weight protamine (LMWP) coupled to the quencher dye QSY21. The self-assembly of this nanoprobe is facilitated by the electrostatic contact between negatively charged heparin and positively charged protamine. The design's reasoning is based on the overexpression of MMP2, which cleaves the protamine peptide sequence upon the probe's arrival to the tumor, thereby detaching the quencher dye and activating the nanoprobe. In vivo experiments utilizing a transferrin receptor peptide (T7)-targeted nanoprobe in an orthotopic glioma mouse model exhibited a significant increase in fluorescence intensity over a 10-hour duration post-injection, validating effective blood-brain barrier penetration and MMP2 activation within the tumor [58]. This nanoprobe design utilized MMPs to cleave peptides that connect cyanine, separating the quencher (gold) from cyanine, thus activating the fluorescent characteristics of cyanine in the tumor's acidic environment and enabling subsequent photothermal therapy. To evaluate the system's dependence on MMP overexpression and pH, two cohorts of nude mice with subcutaneous SCC7 tumors were administered the nanocomposite alongside either an intratumoral injection of an MMP inhibitor or NaHCO3. Fluorescence signals markedly decreased in both groups, validating the dual-responsive characteristics of the nanocomposite. Nonetheless, the overexpression of MMP or downregulation of tissue inhibitor of metalloproteinases (TIMP) resulted in matrix disintegration, cleavage of growth factor receptors, and epithelial-mesenchymal transition (EMT) [59]. Leveraging the elevated expression of ADAM8 in triple-negative breast cancer (TNBC) cells, a strategy incorporating thermosensitive liposomes (LipTS–GD) and targeted delivery through an anti-ADAM8 antibody (MAB1031) was implemented to augment the intracellular uptake of cytotoxic agents for concurrent ultra-high-field MRI (UHF-MRI) and therapeutic intervention. Fluorescence microscopy demonstrated that, after LipTS–GD–MAB therapy, selective binding and doxorubicin release induced a markedly enhanced cytotoxic impact at the targeted cellular site [60].

Mesenchymal Stromal/Stem Cells (MSCs/CSCs)

Mesenchymal stromal cells (MSCs) are multipotent cells with the ability to migrate from the bone marrow to tumor locations due to their tumor-homing properties. Tumor-associated MSCs (TA-MSCs) are mesenchymal stem cells that have assimilated into the tumor microenvironment (TME) due to soluble factors secreted by tumor cells and cancer-associated fibroblasts (CAFs), such as CXCL12, CXCL16, CCL2, CCL5, and TGFβ [61]. Recent studies have underscored the pathogenic functions of TA-MSCs in promoting cancer cell proliferation, migration, and resistance to anticancer therapies, resulting in the formulation of novel therapeutic and imaging approaches aimed at these cells [62]. Nonetheless, obstacles persist, chiefly owing to the absence of distinct cell surface indicators for TA-MSCs, hindering their precise therapeutic modulation. Nevertheless, promising strategies are being investigated as potential therapeutic targets, including the inhibition of chemokines and growth factors derived from TA-MSCs that promote cancer cell proliferation, survival, and angiogenesis, as well as the suppression of chemokines critical for the tumor-specific homing of TA-MSCs. Numerous biomarkers have been identified in relation to cancer stem cells (CSCs), including CD44, CD133, CD90, EpCAM, and ALDH. CD44, a transmembrane adhesion glycoprotein, engages with hyaluronic acid (HA) and is crucial in modulating tumor initiation and proliferation, establishing it as a significant surface biomarker for cancer stem cells (CSCs). The overexpression of CD44 has been associated with the progression of multiple malignancies, such as glioma, ovarian, and lung cancers [63].

Due to its overexpression in various malignancies, CD44 is a viable target for molecular imaging. Karakoçak et al. engineered hyaluronic acid-coated nitrogen-doped quantum dots (HA-nQDs) to mitigate the cytotoxicity of quantum dots while specifically targeting CD44 on tumor cells. Despite HA-nQDs exhibiting reduced efficiency relative to conventional nQDs, they yet displayed enough fluorescence and a robust signal-to-noise ratio when delivered both locally and systemically in mice implanted with patient-derived breast cancer tissue. These results promote additional investigation of HA-nQDs for targeted imaging or drug delivery applications [64]. CD133, a five-transmembrane glycoprotein initially discovered in neuroepithelial stem cells and hematopoietic progenitor cells, is a notable target for cancer stem cells (CSCs). Recent research indicate that CD133 is expressed in multiple malignancies, including liver, pancreatic, breast, and ovarian cancers. Researchers have created advanced imaging agents and tracers that target CD133 to facilitate non-invasive identification of cancer stem cells in these malignancies. Hu et al. created a stable peptidic tracer, [64Cu]Cu-CM-2, that selectively binds to CD133. PET imaging in Huh-7 tumor-bearing mice revealed tracer uptake and retention in the tumors, with the peak tumor-to-blood ratio seen 18 hours post-injection and the highest tumor-to-muscle ratio at 6 hours post-injection [69]. An RNA aptamer directed against CD133 was coupled with cationic liposomes containing siRNA and paclitaxel. This method effectively triggered apoptosis in glioma stem cells and facilitated the differentiation of CD133+ glioma stem cells into non-stem cells, consequently enhancing overall survival in glioma tumor-bearing mice [70].

CD90 is a recognized surface marker of cancer stem cells (CSCs) across various malignancies, including lung cancer [71], ovarian cancer [72], glioblastoma [73], and liver cancer [74]. The expression of CD90 is closely associated with the initiation, progression, metastasis, and resistance to therapy in liver cancer [75]. An innovative study by An et al. focused on the development of anti-CD90 single-chain variable fragment (scFv)-conjugated

microbubbles (MB-CD90-scFv) aimed at the early detection of pancreatic ductal adenocarcinoma (PDAC). The CD90-scFv recombinant fragment was engineered with a cysteine residue at its C-terminus, enabling thioether conjugation to PEGylated microbubbles functionalized with maleimide groups. This conjugation facilitated the binding of the microbubbles to CD90-overexpressing MS1 cells (pancreatic islet endothelial cells) in vitro. In vivo assessments were conducted in a transgenic mouse model of PDAC and in control models with either normal pancreas or pancreatitis induced by l-arginine. The results revealed that MB-CD90-scFv significantly enhanced the ultrasound (US) signal by 4.4-fold compared to non-targeted microbubbles in PDAC tumors. In contrast, mice with normal pancreas or pancreatitis displayed substantially lower US signals compared to those with PDAC, indicating the specificity of MB-CD90-scFv for PDAC detection [76].

Aldehyde dehydrogenases (ALDHs) are established biomarkers for CSCs in various cancers, including lung [77], prostate [78], esophageal [79], and ovarian cancers [80]. Elevated ALDH expression and activity are indicative of increased metastatic potential and poor prognosis. Specifically, the higher activity of the ALDH1A1 isozyme has been linked to chemotherapy resistance and adverse outcomes in colon, ovarian, breast, lung, and prostate cancers, establishing ALDH1A1 as a potential target for cancer therapy and imaging [81]. The fluorescent probe AlDeSense was developed to detect ALDH1A1 activity. In the absence of ALDH1A1, the probe emits weak fluorescence due to the quenching effect of donor-photo-induced electron transfer (d-PeT). However, when ALDH1A1 hydrolyzes the methyl acetate group of AlDeSense, followed by the oxidation of the aldehyde group to a carboxylic acid, the d-PeT effect is disrupted, leading to a 20-fold increase in fluorescence signals compared to the control probe (Ctrl-AlDeSense). Fluorescence imaging in BALB/c mice with e-CSCs showed significantly higher fluorescence in the e-CSC tumors compared to non-CSCs, indicating that e-CSCs were more aggressive and tumorigenic. These findings suggest that AlDeSense can serve as a valuable tool for detecting ALDH1A1 activity in cancer stem cells and for evaluating their aggressiveness and tumorigenic potential [82].

Tumor Immune Microenvironment (TIME)

The tumor microenvironment (TME) is a dynamic ecosystem characterized by the influx of diverse immune cells from both innate and adaptive immune systems, each capable of differentiating and polarizing into distinct phenotypes. Innate immune responses are mediated by cells including natural killer (NK) cells, tumor-associated neutrophils, tumor-associated macrophages, monocytes, eosinophils, mast cells, and myeloid-derived suppressor cells. Conversely, the adaptive immune system encompasses dendritic cells (DCs), along with T and B lymphocytes. Cytotoxic CD8+ T cells and NK cells are essential in coordinating anti-tumor immune responses. Naive T cells are primed and educated by antigen-presenting cells (APCs), especially mature dendritic cells (DCs), in lymph nodes or organized tertiary lymphoid structures near or within tumor tissue. The activated CD8+ T cells subsequently traverse to the inflamed tumor microenvironment, where they identify and eliminate tumor cells in an antigen-specific fashion, releasing cytotoxic agents such as perforin and granzyme. CD4+ T helper (Th1) cells enhance the anti-tumor efficacy of CD8+ T cells by the secretion of cytokines such as IL-2, TNFα, IFNγ, and GM-CSF, which are essential for T cell proliferation and efficient targeting of tumor cells. CD4+ Th2 cells that secrete IL-4, IL-5, and IL-13, together with CD4+ Th1 cells that release IL-17A, IL-17F, IL-21, and IL-22, are generally linked to pro-tumorigenic effects. Regulatory T cells (Tregs), identified by the expression of CD25 and FOXP3, facilitate tumor growth by inhibiting cytotoxic CD8+ T cell activity through the release of immunosuppressive IL-10 and the control of antigen-presenting cell function via CTLA-4–CD80/86 interactions. Molecular imaging is essential for seeing and characterizing immune cells in the tumor microenvironment (TME). A range of immunoPET tracers has been created to target immune cell markers on T cells, B cells, macrophages, myeloid cells, and NK cells. Principal markers for T lymphocytes comprise CD3, CD4, and CD8. CD3, a protein complex present on T cells, is essential for the activation of T helper and cytotoxic T cells. Bispecific antibodies are designed to target CD3, either redirecting T lymphocytes to tumor cells or inducing a cytolytic synapse that releases perforin and granzyme-B to promote cancer cell killing. ERY974 is a bispecific antibody that simultaneously targets CD3 and glypican-3 (GPC3), an oncofetal protein with restricted expression in normal adult tissues [84]. Clinical trials documented on ClinicalTrials.gov indicate that ERY974 has been assessed for the treatment of solid tumors and hepatocellular carcinoma. A study examining the biodistribution of the [89Zr]Zr-N-suc-Df-ERY974 tracer in immunodeficient mice and those engrafted with human immune cells demonstrated more tracer uptake in the latter group. Furthermore, CD3-positive lymphoid tissues, including the mesenteric nodes and spleen, demonstrated the second-highest uptake after tumor uptake, with the liver also exhibiting significant uptake [91]. Subsequent research has examined the biodistribution of bispecific antibodies that target both CD3 and human/mouse EpCAM in immunodeficient and immunocompetent murine models. These investigations similarly observed increased tumor uptake in immunocompetent animals vs to immunodeficient mice. Significantly, EpCAM exerted a more pronounced effect on the biodistribution of [89Zr]Zr-DFO-N-suc-muS110 compared to CD3 [92]. The bispecific monoclonal antibody PF-07062119, which targets CD3 and guanylyl cyclase C (a protein overexpressed in colorectal cancer), has undergone evaluation in a clinical trial for colorectal cancer [93]. Another work utilized an immunoPET tracer targeting CD8, specifically [89Zr]Zr-Df-IAB22M2C, to monitor CD8-positive T cells in a human colorectal cancer adoptive transfer paradigm. The findings indicated a markedly greater absorption of the tracer in mice administered PF-07062119 relative to the control group. The tracer's absorption in tumors exhibited a moderate correlation with CD8 T cell density, validating its utility as a measure for evaluating the therapeutic response to immunotherapy [94]. The application of targeted molecular imaging to assess responses to immunotherapeutic drugs has gained significant prominence. An anti-CD8 cys-diabody tracer labeled with zirconium-89 was utilized to evaluate the effectiveness of oncolytic herpes simplex virus (oHSV) M002 in immunocompetent mice implanted with GSC005 glioma cells. oHSV is an immunotherapeutic approach that

specifically targets tumor cells by multiplying within them. The research entailed the intratumoral administration of oHSV M002 in murine models, succeeded by the injection of [89Zr]Zr-malDFO-169 cys-diabody. The research revealed significantly elevated SUV in tumors subjected to oHSV M002 in contrast to the control group. The absorption of the tracer was additionally diminished when unlabeled cys-diabodies and [89Zr]Zr-antiCD8 cys-diabody were co-administered, particularly in the spleen. Furthermore, the brain-to-blood ratio was markedly elevated in the GSC005 + M002 group (0.15 ± 0.08) in contrast to the blocked experiment group (0.05 ± 0.02) [95].

T helper cells that express the CD4 marker have been employed for targeted imaging of the tumor microenvironment (TME). A nanobody targeting CD4 was conjugated with copper-64 utilizing BCN-NODAGA as the chelating agent. The identical nanobody was utilized for fluorescence imaging through conjugation with Cy5.5 dye. In vivo fluorescence imaging in NOD SCID gamma mice administered CD4+ leukemia cells demonstrated enhanced target accumulation and superior selectivity relative to the control group (GFP-Nb-Cy5.5) [96]. Additionally, the [64Cu]Cu-CD4-Nb1 was evaluated in xenograft mouse models using PET/MRI imaging, conducted 10 minutes post-initial uptake. The tracer was then excreted by the kidneys. The concentration of [64Cu]Cu-CD4-Nb1 in lymphoid nodes, spleen, thymus, and liver was observed to be greater in the human CD4-positive cell model, which contains CD4 T helper cells, compared to wild-type mice [96].

Programmed death-ligand 1 (PD-L1), an immune checkpoint molecule from the immune-regulatory ligand family, is overexpressed in human malignancies and correlates with unfavorable prognosis. PD-L1 is recognized for augmenting the apoptosis of cytotoxic CD8+ T cells through its interaction with PD-1. Immune checkpoint inhibition (ICI) treatments, targeting either PD-L1 or PD-1, seek to avert T-cell apoptosis mediated by PD-L1. FDA-sanctioned anti-PD-L1 monoclonal antibodies, including durvalumab, avelumab, and atezolizumab, provide significant survival enhancements compared to conventional treatments for a limited group of patients. Nonetheless, most respondents do not derive substantial benefits from these therapy, underscoring the pressing necessity for improved predictors of response. The diversity in PD-1/PD-L1 expression levels among patients' tumor microenvironments has heightened interest in imaging PD-1/PD-L1 expressing immune cells. Numerous clinical trials cataloged on clinicaltrials.gov have evaluated radiotracers aimed at PD-1 or PD-L1, including [64Cu]Cu-DOTA-pembrolizumab, [89Zr]Zr-pembrolizumab, [68Ga]Ga-WL12 (a PD-L1-targeting peptide), and [99mTc]Tc-NM01 (a single-domain antibody targeting PD-1) for the detection of solid tumors and lung cancer. Furthermore, Li and associates examined the biodistribution of zirconium-89-labeled pembrolizumab in healthy cynomolgus monkeys. They linked pembrolizumab with tetrafluorophenol-N-succinyl desferal-Fe(III) ester (TFP-N-sucDf) and radiolabeled it using zirconium-89. The biodistribution research of [89Zr]Zr-N-sucDf-pembrolizumab demonstrated a progressive accumulation in lymphoid organs, including the spleen, tonsils, and mesenteric lymph nodes. Nonetheless, non-lymphoid tissues such as the liver, kidney, brain, lung, muscle, and heart exhibited inadequate tracer dispersion. Co-administration of a high dose of pembrolizumab with [89Zr]Zr-N-sucDf-pembrolizumab resulted in reduced uptake in the tonsils, spleen, and lymph nodes, signifying target-mediated accumulation [98].

Notwithstanding the encouraging outcomes from radiolabeled PET probes with anti-PD-L1 antibodies, a hurdle persists due to leftover therapeutic antibodies competing with radiotracers for binding at the target region, which may complicate post-treatment imaging. To mitigate potential saturation effects, Bansal et al. employed a new anti-PD-L1-B11 clone antibody that targets a distinct epitope of PD-L1, in contrast to existing therapeutic antibodies. In a breast cancer tumor model, the [89Zr]Zr-DFO-NCS-anti-PD-L1-B11 clone demonstrated greater uptake in PD-L1-expressing tumors compared to [89Zr]Zr-DFO-NCS-atezolizumab [99]. Additional immune suppressive mechanisms are being investigated to avert tumor evasion. The ITIM domain receptor TIGIT and T cell Ig exemplify such checkpoint inhibitors. TIGIT is an inhibitory receptor found on natural killer cells, CD4+ T lymphocytes, CD8+ cytotoxic T lymphocytes, and FOXP3+ regulatory T lymphocytes. A study utilized a TIGIT-targeting antibody-based radiotracer that was radiolabeled with copper-64 and zirconium-89. PET imaging of TIGIT-expressing cancer cell-bearing xenografts and syngeneic animal models exhibited enhanced contrast with the zirconium-89-labeled tracer in comparison to the copper-64-labeled tracer. The disparity is probably attributable to enhanced alignment with antibody pharmacokinetics and reduced circulation clearance of 89Zr, facilitating more distinct imaging of TIGIT-expressing malignancies [100]. Cytokines and chemokines, with cell markers and immunological checkpoint molecules, are being intensively targeted for cancer molecular imaging. Chemokines, tiny peptides of 8–10 kDa containing two or four cysteine residues, are essential for immune system control and homeostasis, although they can also be linked to numerous malignancies and inflammatory illnesses. Chemokines are categorized into four groups according to the arrangement of their cysteine residues: CC, CXC, CX3C, and XC [101]. Pentixafor, a chemical recognized for its interaction with the CXCR4 binding site, is well-established for oncological imaging applications. A new study utilized gallium-68-labeled pentixafor to assess bone marrow involvement in myeloproliferative neoplasms among 12 individuals. The results indicated increased tracer uptake in the bone marrow and hematopoietic regions compared to the controls. Moreover, individuals administered ruxolitinib or hydroxyurea subsequent to initial PET imaging with [68Ga]Ga-DOTA-pentixafor had reduced tracer uptake in the bone marrow and spleen upon follow-up PET scans at the 6-month mark, signifying a treatment response. [68Ga]Ga-DOTA-pentixafor has undergone assessment in many clinical trials concerning non-Hodgkin lymphoma, multiple myeloma, and other hematologic malignancies.

Moreover, researchers focused on CCR2 utilizing a peptide, EC1i, conjugated with gold nanoclusters and tagged with copper-64. This tracer was developed to evaluate CCR2 expression in triple-negative breast (TNB) cancer, which correlates with unfavorable prognosis. In vivo PET imaging of 4T1 TNB cancer-bearing mice demonstrated significant tumoral accumulation of [64Cu]Cu-AuNCs-EC1i one week after injection. The tracer's specificity was further validated by co-injecting unlabeled EC1i, leading to a 41% decrease in tumor uptake. The tracer was swiftly eliminated from the bloodstream by

renal excretion, exhibiting negligible background radioactivity in non-target tissues, including the liver [103]. The cytokine interleukin-2 (IL-2), with a molecular weight of 15 kDa, is crucial for T cell development, proliferation, activation, and differentiation through its interaction with IL-2 receptors (IL-2Rs). The high-affinity IL-2 receptor (CD25) is mostly present on regulatory T cells (Tregs) and activated effector T cells, whereas the low-affinity IL-2 receptor, consisting of CD132 and CD122, is more prevalent in natural killer (NK) and naïve T cells. Tumor-specific T cells inside the tumor microenvironment are essential for forecasting the efficacy of immune checkpoint inhibitor therapy. Consequently, seeing these T cells within the tumor microenvironment provides critical insights on anti-tumor immune responses and the possible advantages of immune checkpoint inhibitors. The 18F-labeled IL-2 PET tracer ([18F]-FB-IL2) has been extensively studied. Clinical investigations have evaluated the pharmacokinetics and biodistribution of [18F]-FB-IL2, including its application in PET imaging for patients with metastatic melanoma to detect immunological responses generated by immune checkpoint inhibitors. Although [18F]-FB-IL2 PET imaging effectively visualizes both immunostimulatory and immunosuppressive cells within the tumor microenvironment, uptake in melanoma patients was suboptimal due to diminished CD25 expression in tumors and increased expression in regulatory T cells following immune checkpoint inhibitor therapy. An alternate strategy has been suggested to target the low-binding affinity IL-2R (CD122/γc) by obstructing IL-2 binding to CD25 through the creation of IL-2/anti-IL-2 complexes (IL-2c) using monoclonal antibodies like S4B6. This technique extends IL-2 circulation and facilitates the monitoring of both cytotoxic CD8+ T cells and NK cells, while suppressing Tregs [104].

Natural killer (NK) cells, as innate cytotoxic lymphocytes, can identify and eradicate tumor cells in an antigen-independent fashion, especially when tumor cells downregulate major histocompatibility complex class I (MHC-I) molecules, crucial for antigen presentation. Natural killer (NK) cells eliminate tumor cells by antibody-dependent cell-mediated cytotoxicity (ADCC) and direct cytotoxicity, while also influencing anti-tumor immune responses through the secretion of cytokines and chemokines [105, 106]. ADCC transpires when CD16, a surface receptor inherently present on NK cells, attaches to the Fc region of an antibody [108]. The activity of NK cells is regulated by the equilibrium between activating NK receptors (aNKRs) and inhibitory NK receptors (iNKRs) that identify tumor-associated chemicals. Zeng et al. conducted a study in which they radiolabeled an anti-NK1.1 antibody, targeting the NK cell surface marker, with iodine-124 ([124I]I-NK1.1), and assessed its efficacy in imaging NK cells in tumor-bearing animals using PET. [124I]I-NK1.1 PET imaging showed selective targeting and enhanced tumor uptake in NK1.1+ tumor xenografts relative to controls, with notable retention in NK1.1+ tissues including the spleen, bone marrow, and liver. The tracer was efficiently eliminated by the kidneys, and its tumor-to-muscle ratio was determined to be superior to that of other imaging agents [107]. Alternative methodologies for NK cell imaging have included the creation of small molecule ligands for the visualization and targeting of NK cells via optical and radiolabeled probes. A work by Kegley et al. focused on creating a radiolabeled small chemical that targets the NK cell receptor NKG2D, which plays a role in identifying stress-induced ligands on tumor cells. NKG2D-targeting small compounds have been radiolabeled with fluorine-18 to visualize NK cells in the tumor microenvironment. This method improves the specificity and sensitivity of imaging, facilitating a more precise evaluation of NK cell-mediated anti-tumor immunity and optimizing immunotherapeutic approaches [109]. In summary, molecular imaging of immune cells and checkpoint markers holds considerable promise for advancing our comprehension of tumor-immune interactions and refining the assessment of immunotherapies. Utilizing radiolabeled tracers to target specific immune cells, immunological checkpoints, and cytokines can yield critical insights into treatment responses, inform therapeutic decisions, and forecast patient outcomes [110].

Conclusion:

The tumor microenvironment (TME) is a multifaceted ecosystem that significantly influences cancer progression, metastasis, and therapeutic responses. Its complexity arises from the diverse cellular and non-cellular components, such as cancer-associated fibroblasts (CAFs), immune cells, blood vessels, and the extracellular matrix (ECM), which interact dynamically to support tumor growth. The functional heterogeneity of these components is evident not only between different cancer types but also within individual tumors. This variation complicates the development of effective treatment strategies, emphasizing the importance of understanding the TME's evolving role at various stages of cancer progression. Recent advancements in imaging technologies have facilitated the detection and monitoring of TME components, providing valuable insights into tumor behavior. Biomarkers like fibroblast activation protein (FAP), collagen, and fibronectin have emerged as promising targets for imaging, with radiotracers such as [68Ga]Ga-FAPI-04 and [68Ga]Ga-FAPI-46 demonstrating superior diagnostic accuracy. These biomarkers help identify critical aspects of the TME, such as stromal remodeling, immune infiltration, and angiogenesis, which are crucial for tumor survival and spread. Furthermore, molecular imaging of the TME has shown potential in predicting tumor response to treatments like chemotherapy and radiation therapy, thus enabling more personalized therapeutic approaches. While molecular imaging holds great promise, challenges remain in optimizing imaging agents for clinical use. Issues such as rapid clearance and suboptimal tumor retention of radiotracers need to be addressed to improve diagnostic and therapeutic efficacy. Recent innovations, such as the development of modified radiotracers conjugated with albumin binder-truncated Evans blue, show promise in overcoming these limitations and enhancing tumor-specific accumulation. In conclusion, the ability to visualize and analyze the tumor microenvironment in vivo provides a powerful tool for advancing cancer diagnosis, staging, and treatment monitoring. Continued research into the molecular components of the TME and the development of more effective imaging agents will play a crucial role in the future of precision oncology. Furthermore, the integration of TME-targeted imaging into clinical practice could lead to more accurate tumor profiling, better treatment selection, and ultimately, improved patient outcomes.

References:

1. Aghanejad A, Bonab SF, Sepehri M et al (2022) A review on targeting tumor microenvironment: the main paradigm shift in the mAb-based immunotherapy of solid tumors. Int J Biol Macromol 207:592–610
2. Simon T, Salhia B (2022) Cancer-associated fibroblast subpopulations with diverse and dynamic roles in the tumor microenvironment. Mol Cancer Res 20:183–192
3. Asgari D, Aghanejad A, Mojarrad JS (2011) An improved convergent approach for synthesis of erlotinib, a tyrosine kinase inhibitor, via a ring closure reaction of phenyl benzamidine intermediate. Bull Korean Chem Soc 32:909–914
4. Nabi PN, Vahidfar N, Tohidkia MR, Hamidi AA, Omidi Y, Aghanejad A (2021) Mucin-1 conjugated polyamidoamine-based nanoparticles for image-guided delivery of gefitinib to breast cancer. Int J Biol Macromol 174:185–197
5. Byrne NM, Tambe P, Coulter JA (2021) Radiation response in the tumour microenvironment: predictive biomarkers and future perspectives. J Personalized Med 11:53
6. Duan J, Lv G, Zhu N et al (2022) Multidimensional profiling depicts infiltrating immune cell heterogeneity in the tumor microenvironment of stage IA non-small cell lung cancer. Thoracic Cancer 13:947–955
7. Kadkhoda J, Akrami-Hasan-Kohal M, Tohidkia MR, Khaledi S, Davaran S, Aghanejad A (2021) Advances in antibody nanoconjugates for diagnosis and therapy: a review of recent studies and trends. Int J Biol Macromol 185:664–678
8. Wei R, Liu S, Zhang S, Min L, Zhu S (2020) Cellular and extracellular components in tumor microenvironment and their application in early diagnosis of cancers. Anal Cell Pathol 2020:6283796
9. Vahidfar N, Eppard E, Farzanehfar S, Yordanova A, Fallahpoor M, Ahmadzadehfar H (2021) An impressive approach in nuclear medicine: theranostics. PET Clin 16:327–340
10. Mirzaei A, Jalilian AR, Aghanejad A et al (2015) Preparation and evaluation of 68Ga-ECC as a PET renal imaging agent. Nucl Med Mol Imaging 49:208–216
11. Aghanejad A, Jalilian AR, Maus S, Yousefnia H, Geramifar P, Beiki D (2016) Optimized production and quality control of 68Ga-DOTATATE. Iran J Nucl Med 24:29–36
12. Chen Q, Chen AZ, Jia G, Li J, Zheng C, Chen K (2022) Molecular imaging of tumor microenvironment to assess the effects of locoregional treatment for hepatocellular carcinoma. Hepatology Communications 6:652–664
13. Vahidfar N, Aghanejad A, Ahmadzadehfar H, Farzanehfar S, Eppard E (2021) Theranostic advances in breast cancer in nuclear medicine. Int J Mol Sci 22(9):4597. https://doi.org/10.3390/ijms22094597
14. Nicin L, Wagner JUG, Luxán G, Dimmeler S (2022) Fibroblast-mediated intercellular crosstalk in the healthy and diseased heart. FEBS Lett 596:638–654
15. Moretti L, Stalfort J, Barker TH, Abebayehu D (2022) The interplay of fibroblasts, the extracellular matrix, and inflammation in scar formation. J Biol Chem 298(2):101530
16. Poon S, Ailles LE (2022) Modeling the role of cancer-associated fibroblasts in tumor cell invasion. Cancers 14:962
17. Chen Y, McAndrews KM, Kalluri R (2021) Clinical and therapeutic relevance of cancer-associated fibroblasts. Nat Rev Clin Oncol 18:792–804
18. Li M, Younis MH, Zhang Y, Cai W, Lan X (2022) Clinical summary of fibroblast activation protein inhibitor-based radiopharmaceuticals: cancer and beyond. Eur J Nucl Med Mol Imaging 49(8):2844–2868
19. Lindner T, Loktev A, Altmann A et al (2018) Development of quinoline-based theranostic ligands for the targeting of fibroblast activation protein. J Nucl Med 59:1415–1422
20. Guo W, Pang Y, Yao L et al (2021) Imaging fibroblast activation protein in liver cancer: a single-center post hoc retrospective analysis to compare [68Ga]Ga-FAPI-04 PET/CT versus MRI and [18F]-FDG PET/CT. Eur J Nucl Med Mol Imaging 48:1604–1617
21. Jin X, Wei M, Wang S et al (2022) Detecting fibroblast activation proteins in lymphoma using 68Ga-FAPI PET/CT. J Nucl Med: Off Publ Soc Nucl Med 63:212–217
22. Röhrich M, Leitz D, Glatting FM et al (2022) Fibroblast activation protein-specific PET/CT imaging in fibrotic interstitial lung diseases and lung cancer: a translational exploratory study. J Nucl Med 63:127–133
23. Kessler L, Ferdinandus J, Hirmas N et al (2022) 68Ga-FAPI as a diagnostic tool in sarcoma: data from the 68Ga-FAPI PET prospective observational trial. J Nucl Med: Off Publ Soc Nucl Med 63:89–95
24. Backhaus P, Burg MC, Roll W et al (2022) Simultaneous FAPI PET/MRI targeting the fibroblast-activation protein for breast cancer. Radiology 302:39–47
25. Liu Y, Watabe T, Kaneda-Nakashima K et al (2022) Fibroblast activation protein targeted therapy using [177Lu]FAPI-46 compared with [225Ac]FAPI-46 in a pancreatic cancer model. Eur J Nucl Med Mol Imaging 49:871–880
26. Huang J, Fu L, Hu K et al (2022) Automatic production and preliminary PET imaging of a new imaging agent [18F]AlF-FAPT. Front Oncol 11:802676
27. Ruan Q, Feng J, Jiang Y et al (2022) Preparation and bioevaluation of 99mTc-labeled FAP inhibitors as tumor radiotracers to target the fibroblast activation protein. Mol Pharm 19:160–171
28. Wen X, Xu P, Shi M et al (2022) Evans blue-modified radiolabeled fibroblast activation protein inhibitor as long-acting cancer therapeutics. Theranostics 12:422–433
29. Qin C, Liu F, Huang J et al (2021) A head-to-head comparison of 68Ga-DOTA-FAPI-04 and 18F-FDG PET/MR in patients with nasopharyngeal carcinoma: a prospective study. Eur J Nucl Med Mol Imaging 48:3228–3237
30. Holl J, Kowalewski C, Zimek Z et al (2021) Chronic diabetic wounds and their treatment with skin substitutes. Cells 10(3):655
31. Romani P, Nirchio N, Arboit M et al (2022) Mitochondrial fission links ECM mechanotransduction to metabolic redox homeostasis

and metastatic chemotherapy resistance. Nat Cell Biol 24:168–180
32. Liu F, Yan JR, Chen S et al (2020) Polypeptide-rhodamine B probes containing laminin/fibronectin receptor-targeting sequence (YIGSR/RGD) for fluorescent imaging in cancers. Talanta 212:120718
33. Zunder SM, Gelderblom H, Tollenaar RA, Mesker WE (2020) The significance of stromal collagen organization in cancer tissue: an in-depth discussion of literature. Crit Rev Oncol/Hematol 151:102907
34. Erstad DJ, Sojoodi M, Taylor MS et al (2020) Fibrotic response to neoadjuvant therapy predicts survival in pancreatic cancer and is measurable with collagen-targeted molecular MRI. Clin Cancer Res 26:5007–5018
35. Bennink LL, Li Y, Kim B et al (2018) Visualizing collagen proteolysis by peptide hybridization: from 3D cell culture to *in vivo* imaging. Biomaterials 183:67–76
36. Dalton CJ, Lemmon CA (2021) Fibronectin: molecular structure, fibrillar structure and mechanochemical signaling. Cells 10(9):2443
37. Qiao PL, Gargesha M, Liu Y et al (2022) Magnetic resonance molecular imaging of extradomain B fibronectin enables detection of pancreatic ductal adenocarcinoma metastasis. Magn Reson Imaging 86:37–45
38. Wei J, Hu M, Huang K, Lin S, Du H (2020) Roles of proteoglycans and glycosaminoglycans in cancer development and progression. Int J Mol Sci 21:1–28
39. Faria-Ramos I, Poças J, Marques C et al (2021) Heparan sulfate glycosaminoglycans: (un)expected allies in cancer clinical management. Biomolecules 11:1–28
40. Huang X, Fan C, Zhu H et al (2018) Glypican-1-antibody-conjugated Gd–Au nanoclusters for FI/MRI dual-modal targeted detection of pancreatic cancer. Int J Nanomed 13:2585–2599
41. Lingasamy P, Laarmann AH, Teesalu T (2021) Tumor penetrating peptide-functionalized tenascin-C antibody for glioblastoma targeting. Curr Cancer Drug Targets 21:70–79
42. Kumazoe M, Hiroi S, Tanimoto Y et al (2020) Cancer cell selective probe by mimicking EGCG. Biochem Biophys Res Commun 525:974–981
43. Cai X, Wei W, Liu Z, Bai Z, Lei J, Xiao J (2020) In situ imaging of pathological collagen by electrostatic repulsion-destabilized peptide probes. ACS Appl Bio Mater 3:7492–7499
44. Salarian M, Yang H, Turaga RC et al (2019) Precision detection of liver metastasis by collagen-targeted protein MRI contrast agent. Biomaterials 224:119478
45. Yao D, Wang Y, Zou R et al (2021) Wavelength-adjustable butterfly molecules in dynamic nanoassemblies for extradomain-B fibronectin-modulating optical imaging and synchronous phototherapy of triple-negative breast cancer. Chem Eng J 420:127658
46. Schilb AL, Ayat NR, Vaidya AM et al (2021) Efficacy of targeted ECO/miR-200c nanoparticles for modulating tumor microenvironment and treating triple negative breast cancer as non-invasively monitored by MR molecular imaging. Pharm Res 38:1405–1418
47. Wang Y, Jiang L, Zhang Y et al (2020) Fibronectin-targeting and cathepsin B-activatable theranostic nanoprobe for MR/fluorescence imaging and enhanced photodynamic therapy for triple negative breast cancer. ACS Appl Mater Interfaces 12:33564–33574
48. Tseng WB, Chou YS, Lu CZ, Madhu M, Lu CY, Tseng WL (2021) Fluorescence sensing of heparin and heparin-like glycosaminoglycans by stabilizing intramolecular charge transfer state of dansyl acid-labeled AG73 peptides with glutathione-capped gold nanoclusters. Biosens Bioelectron 193:113522
49. Sugyo A, Tsuji AB, Sudo H, Takano K, Kusakabe M, Higashi T (2020) Proof of concept study for increasing tenascin-C-targeted drug delivery to tumors previously subjected to therapy: X-irradiation increases tumor uptake. Cancers 12:1–15
50. Lu Z, Kamat K, Johnson BP, Yin CC, Scholler N, Abbott KL (2019) Generation of a fully human scFv that binds tumor-specific glycoforms. Sci Rep 9:1–11
51. Pereira PMR, Ragupathi A, Shmuel S, Mandleywala K, Viola NT, Lewis JS (2019) HER2-targeted PET imaging and therapy of hyaluronan- masked HER2-overexpressing breast cancer affiliations: Department of Oncology. Wayne State University, Molecular Pharmacology Program, Memorial Sloan Kettering Cancer Center, Karmanos Cancer Institute
52. Łukaszewicz-Zając M, Dulewicz M, Mroczko B (2021) A disintegrin and metalloproteinase (ADAM) family: their significance in malignant tumors of the central nervous system (CNS). Int J Mol Sci 22(19):10378
53. Fischer T, Riedl R (2021) Challenges with matrix metalloproteinase inhibition and future drug discovery avenues. Expert Opin Drug Discov 16:75–88
54. Umeizudike K, Räisänen I, Gupta S et al (2022) Active matrix metalloproteinase-8: a potential biomarker of oral systemic link. Clin Exp Dent Res 8:359–365
55. Kaasinen M, Hagström J, Mustonen H et al (2022) Matrix metalloproteinase 8 expression in a tumour predicts a favourable prognosis in pancreatic ductal adenocarcinoma. Int J Mol Sci 23(6):3314
56. Nikolov A, Popovski N (2021) Role of gelatinases MMP-2 and MMP-9 in healthy and complicated pregnancy and their future potential as preeclampsia biomarkers. Diagnostics 11:480
57. Jiang H, Li H (2021) Prognostic values of tumoral MMP2 and MMP9 overexpression in breast cancer: a systematic review and meta-analysis. BMC Cancer 21:149
58. Yin L, Sun H, Zhao M et al (2019) Rational design and synthesis of a metalloproteinase-activatable probe for dual-modality imaging of metastatic lymph nodes *in vivo*. J Org Chem 84(10):6126–6133
59. Winer A, Adams S, Mignatti P (2018) Matrix metalloproteinase inhibitors in cancer therapy: turning past failures into future successes. Mol Cancer Ther 17:1147–1155
60. Alawak M, Abu Dayyih A, Mahmoud G et al (2021) ADAM 8 as a novel target for doxorubicin delivery to TNBC cells using magnetic thermosensitive liposomes. Eur J Pharm Biopharm 158:390–400

61. Raza S, Rajak S, Tewari A et al (2022) Multifaceted role of chemokines in solid tumors: from biology to therapy. Semin Cancer Biol 86(Pt 3):1105–1121
62. Luo T, von der Ohe J, Hass R (2021) MSC-derived extracellular vesicles in tumors and therapy. Cancers 13(20):5212
63. Xu H, Niu M, Yuan X, Wu K, Liu A (2020) CD44 as a tumor biomarker and therapeutic target. Exp Hematol Oncol 9:1–14
64. Karakoçak BB, Laradji A, Primeau T, Berezin MY, Li S, Ravi N (2021) Hyaluronan-conjugated carbon quantum dots for bioimaging use. ACS Appl Mater Interfaces 13:277–286
65. Barghi L, Aghanejad A, Valizadeh H, Barar J, Asgari D (2012) Modified synthesis of erlotinib hydrochloride. Adv Pharm Bull 2:119–122
66. Hori Y (2013) Prominin-1 (CD133) reveals new faces of pancreatic progenitor cells and cancer stem cells: current knowledge and therapeutic perspectives. Adv Exp Med Biol 777:185–196
67. Aghanejad A, Jalilian AR, Fazaeli Y et al (2014) Synthesis and evaluation of [67Ga]-AMD3100: a novel imaging agent for targeting the chemokine receptor CXCR4. Sci Pharm 82:29–42
68. Srivastava M, Ahlawat N, Srivastava A (2021) Ovarian cancer stem cells: newer horizons. J Obstet Gynecol India 71:115–117
69. Hu K, Ma X, Xie L et al (2022) Development of a stable peptide-based PET tracer for detecting CD133-expressing cancer cells. ACS Omega 7:334–341
70. Sun X, Chen Y, Zhao H et al (2018) Dual-modified cationic liposomes loaded with paclitaxel and survivin siRNA for targeted imaging and therapy of cancer stem cells in brain glioma. Drug Delivery 25:1718–1727
71. Raniszewska A, Kwiecień I, Rutkowska E, Rzepecki P, Domagała-Kulawik J (2021) Lung cancer stem cells—origin, diagnostic techniques and perspective for therapies. Cancers 13(12):2996
72. Dhaliwal D, Shepherd TG (2022) Molecular and cellular mechanisms controlling integrin-mediated cell adhesion and tumor progression in ovarian cancer metastasis: a review. Clin Exp Metas 39:291–301
73. Nowak B, Rogujski P, Janowski M, Lukomska B, Andrzejewska A (2021) Mesenchymal stem cells in glioblastoma therapy and progression: how one cell does it all. Biochimica et Biophysica Acta (BBA) - Reviews on Cancer 1876:188582
74. Yamashita T, Kaneko S (2021) Liver cancer stem cells: recent progress in basic and clinical research. Regenerative Therapy 17:34–37
75. Liu Y-C, Yeh C-T, Lin K-H (2020) Cancer stem cell functions in hepatocellular carcinoma and comprehensive therapeutic strategies. Cells 9(6):1331
76. Bam R, Daryaei I, Abou-Elkacem L et al (2020) Toward the clinical development and validation of a Thy1-targeted ultrasound contrast agent for the early detection of pancreatic ductal adenocarcinoma. Invest Radiol 55:711–721
77. Masciale V, Grisendi G, Banchelli F et al (2020) CD44+/EPCAM+ cells detect a subpopulation of ALDHhigh cells in human non-small cell lung cancer: a chance for targeting cancer stem cells? Oncotarget 11:1545
78. Püschel J, Dubrovska A, Gorodetska I (2021) The multifaceted role of aldehyde dehydrogenases in prostate cancer stem cells. Cancers 13(18):4703
79. Choi CK, Yang J, Kweon S-S et al (2021) Association between ALDH2 polymorphism and esophageal cancer risk in South Koreans: a case-control study. BMC Cancer 21:254
80. Guo F, Yang Z, Sehouli J, Kaufmann AM (2022) Blockade of ALDH in cisplatin-resistant ovarian cancer stem cells *in vitro* synergistically enhances chemotherapy-induced cell death. Current Oncol 29(4):2808–2822
81. Pereira R, Flaherty RL, Edwards RS, Greenwood HE, Shuhendler AJ, Witney TH (2022) A prodrug strategy for the *in vivo* imaging of aldehyde dehydrogenase activity. RSC Chemical Biology 3:561–570
82. Anorma C, Hedhli J, Bearrood TE et al (2018) Surveillance of cancer stem cell plasticity using an isoform-selective fluorescent probe for aldehyde dehydrogenase 1A1. ACS Cent Sci 4:1045–1055
83. Choi S, Lee SH, Park S, Park SH, Park C, Key J (2021) Indocyanine green-loaded plga nanoparticles conjugated with hyaluronic acid improve target specificity in cervical cancer tumors. Yonsei Med J 62:1042–1051
84. Ning J, Jiang S, Li X et al (2021) GPC3 affects the prognosis of lung adenocarcinoma and lung squamous cell carcinoma. BMC Pulm Med 21:199
85. Demir B, Moulahoum H, Ghorbanizamani F et al (2021) Carbon dots and curcumin-loaded CD44-targeted liposomes for imaging and tracking cancer chemotherapy: a multi-purpose tool for theranostics. J Drug Deliv Sci Technol 62:102363
86. Liu Y, Yao X, Wang C et al (2021) Peptide-based 68Ga-PET radiotracer for imaging CD133 expression in colorectal cancer. Nucl Med Commun 42(10):1144–1150
87. Jung KH, Lee JH, Kim M, Lee EJ, Cho YS, Lee KH (2022) Celecoxib-induced modulation of colon cancer CD133 expression occurs through AKT inhibition and is monitored by 89Zr immuno-PET. Mol Imaging 2022:4906934
88. Tan H, Hou N, Liu Y et al (2020) CD133 antibody targeted delivery of gold nanostars loading IR820 and docetaxel for multimodal imaging and near-infrared photodynamic/photothermal/chemotherapy against castration resistant prostate cancer. Nanomed: Nanotechnol Biol Med 27:102192
89. Pan Y, Zhou S, Liu C et al (2022) Dendritic polyglycerol-conjugated gold nanostars for metabolism inhibition and targeted photothermal therapy in breast cancer stem cells. Adv Healthcare Mater 11(8):e2102272
90. Lu Q, Yang M-F, Liang Y-J et al (2022) Immunology of inflammatory bowel disease: molecular mechanisms and therapeutics. J Inflamm Res 15:1825–1844
91. Waaijer SJH, Giesen D, Ishiguro T et al (2020) Preclinical PET imaging of bispecific antibody ERY974 targeting CD3 and glypican 3 reveals that tumor uptake correlates to T cell infiltrate. J Immuno Therapy Cancer 8(1):e000548
92. Suurs FV, Lorenczewski G, Stienen S et al (2020) The biodistribution of a CD3 and EpCAM bispecific T-cell engager is driven by the CD3 arm. J Nucl Med 61:1594–1601

93. Mathur D, Root AR, Bugaj-Gaweda B et al (2020) A novel GUCY2C-CD3 T-cell engaging bispecific construct (PF-07062119) for the treatment of gastrointestinal cancers. Clin Cancer Res 26:2188–2202
94. Maresca KP, Chen J, Mathur D et al (2021) Preclinical evaluation of 89Zr-Df-IAB22M2C PET as an imaging biomarker for the development of the GUCY2C-CD3 bispecific PF-07062119 as a T cell engaging therapy. Mol Imag Biol 23:941–951
95. Kasten BB, Houson HA, Coleman JM et al (2021) Positron emission tomography imaging with 89Zr-labeled anti-CD8 cys-diabody reveals CD8+ cell infiltration during oncolytic virus therapy in a glioma murine model. Sci Rep 11:1–12
96. Traenkle B, Kaiser PD, Pezzana S et al (2021) Single-domain antibodies for targeting, detection, and *in vivo* imaging of human CD4+ cells. Front Immunol 12:1–17
97. Martorana F, Colombo I, Treglia G, Gillessen S, Stathis A (2021) A systematic review of phase II trials exploring anti-PD-1/PD-L1 combinations in patients with solid tumors. Cancer Treat Rev 101:102300
98. Li W, Wang Y, Rubins D et al (2021) PET/CT imaging of 89Zr-N-sucDf-pembrolizumab in healthy cynomolgus monkeys. Mol Imag Biol 23:250–259
99. Bansal A, Pandey MK, Barham W et al (2021) Non-invasive immunoPET imaging of PD-L1 using anti-PD-L1-B11 in breast cancer and melanoma tumor model. Nucl Med Biol 100–101:4–11
100. Shaffer T, Natarajan A, Gambhir SS (2021) PET imaging of TIGIT expression on tumor-infiltrating lymphocytes. Clin Cancer Res 27:1932–1940
101. Alluri SR, Higashi Y, Kil KE (2021) Pet imaging radiotracers of chemokine receptors. Molecules 26:1–22
102. Kraus S, Dierks A, Rasche L et al (2022) 68Ga-Pentixafor PET/CT for detection of chemokine receptor CXCR4 expression in myeloproliferative neoplasms. J Nucl Med: Off Publ Soc Nucl Med 63:96–99
103. Zhao Y, You M, Detering L, Sultan D, Luehmann H, Liu Y (2021) Chemokine receptor 2 targeted gold nanocluster imaging triple negative breast cancer with positron emission tomography. Part Part Syst Charact 38(3):2000287
104. van de Donk PP, Wind TT, Hooiveld-Noeken JS et al (2021) Interleukin-2 PET imaging in patients with metastatic melanoma before and during immune checkpoint inhibitor therapy. Eur J Nucl Med Mol Imaging 48:4369–4376
105. Hess PR (2022) Major histocompatibility complex antigens. In: Brooks MB, Harr KE, Seelig DM, Wardrop KJ, Weiss DJ (eds) Schalm's veterinary hematology. Wiley, pp 48–62. https://doi.org/10.1002/9781119500537.ch7
106. Khajeh S, Tohidkia MR, Aghanejad A, Mehdipour T, Fathi F, Omidi Y (2018) Phage display selection of fully human antibody fragments to inhibit growth-promoting effects of glycine-extended gastrin 17 on human colorectal cancer cells. Artif Cells Nanomed Biotechnol 46:1082–1090
107. Fouladi M, Sarhadi S, Tohidkia M et al (2019) Selection of a fully human single domain antibody specific to Helicobacter pylori urease. Appl Microbiol Biotechnol 103:3407–3420
108. Dixon KJ, Wu J, Walcheck B (2021) Engineering anti-tumor monoclonal antibodies and Fc receptors to enhance ADCC by human NK cells. Cancers 13(2):312
109. Wang Y, Hu Y, Jiang Y, Zhou S (2021) Oxidative stress in the tumor immune microenvironment. In: Huang C, Zhang Y (eds) Oxidative stress: human diseases and medicine. Springer, Singapore, pp 27–54
110. Siminzar, P., Tohidkia, M. R., Eppard, E., Vahidfar, N., Tarighatnia, A., & Aghanejad, A. (2023). Recent trends in diagnostic biomarkers of tumor microenvironment. *Molecular Imaging and Biology*, *25*(3), 464-482.